### Title

Morphological changes of intracranial pressure quantifies vasodilatory effect of verapamil to treat cerebral vasospasm.




### Journal

Journal of NeuroInterventional Surgery, 12(8)



### Authors

Liu, Xiuyun

Gudelunas, Koa

Ho, Nhi

et al.



### Publication Date

2020-08-01

### DOI

10.1136/neurintsurg-2019-015499

Peer reviewed

Published in final edited form as:

*J Neurointerv Surg*. 2020 August ; 12(8): 802–808. doi:10.1136/neurintsurg-2019-015499.

# Morphological Changes of Intracranial Pressure Quantifies Vasodilatory Effect of Verapamil to Treat Cerebral Vasospasm

**Xiuyun Liu, PhD**[1,2], **Jeffrey R. Vitt, MD**[3], **Steven W. Hetts, MD**[4], **Koa Gudelunas, BS**[1], **Nhi Ho, MD**[1], **Nerissa Ko, MD**[3], **Xiao Hu, PhD**[1,5,6,7]

[1]Department of Physiological Nursing, University of California, San Francisco, USA

[2]Department of Anesthesiology and Critical Care Medicine, School of Medicine, The Johns Hopkins University, Baltimore, Maryland, USA

[3]Department of Neurology, University of California, San Francisco, USA

[4]Department of Radiology and Biomedical Imaging, University of California, San Francisco, USA

[5]Department of Neurological Surgery, School of Medicine, UCSF

[6]Department of Neurosurgery, School of Medicine, UCLA

[7]Bakar Computational Health Sciences Institute, UCSF

## Abstract

**Introduction—**After aneurysmal subarachnoid hemorrhage SAH, both proximal and distal cerebral vasospasm can contribute to the development of delayed cerebral ischemia. Intra-arterial (IA) vasodilators are a mainstay of treatment for distal arterial vasospasm, however there are no well-established methods to assess the efficacy of interventions in real-time. This study aims to introduce a new method for continuous intra-procedural assessment of endovascular treatment (EVT) for cerebral vasospasm.

**Methods—**The premise of our approach is that distal cerebral arterial changes induce a consistent pattern in the morphological changes of intracranial pressure (ICP) pulse. This premise was demonstrated using a published algorithm in previous papers. In this study, we applied the algorithm to calculate the likelihood of cerebral vasodilation (VDI) and cerebral vasoconstriction (VCI) from intra-procedural ICP signals that are synchronized with injection of IA vasodilator verapamil. Cerebral blood flow velocities (CBFV) on bilateral cerebral arteries were studied pre and post IA therapy.

**Corresponding Author**: Xiuyun Liu, Department of Physiological Nursing, University of California, San Francisco, CA, 94122, USA liuxiuyun1@gmail.com. Tel:+1 4153192226.

CONTRIBUTORSHIP STATEMENT

XH and SWH conceived and designed the study. XYL, KG, NH, NK collected data. XYL performed data analysis and drafted the manuscript. JRV, XH, SWH, NK, XYL interpreted the data. All authors reviewed the manuscript and approved the submission.

COMPETING INTERESTS STATEMENT

The author(s) declared no potential conflicts of interest with respect to the research, authorship, and/or publication of this article.

DATA SHARING

The data used in this study are available upon reasonable request to Dr Xiuyun Liu (liuxiuyun1@gmail.com).

**Results—**192 recordings of SAH patients were reviewed and 27 recordings have high-quality ICP waveforms. The VCI was significantly lower after the first verapamil injection (0.47 ± 0.017) than VCI at baseline (0.49 ± 0.020, p<0.001). Larger dosage of verapamil injection results in larger and longer VDI increase. CBFV of middle cerebral artery (MCA) increases across days before the injection of verapamil and it decreases after IA therapy.

**Conclusion—**This study provides preliminary validation of an algorithm for continuous assessment of distal cerebral arterial changes in response to IA vasodilator infusion in patients with vasospasm and aneurysmal SAH.

### Keywords

Vasodilator; Endovascular Treatment; Intra-Arterial Treatment; Cerebral Vasospasm; Subarachnoid Hemorrhage

## INTRODUCTION

Aneurysmal subarachnoid hemorrhage (SAH) is a life-threatening neurologic illness which carries a substantially high burden of premature mortality and is responsible for over a quarter of years of life lost due to cerebrovascular disease before the age of 65[1]. For those that survive the initial hemorrhage event, 20–40% of patients experience delayed cerebral ischemia (DCI) within 3–14 days of ictus and this can lead to cerebral infarction and permanent neurologic deficits [2–4]. Intracranial large vessel arterial vasospasm after SAH can lead to regional hypoperfusion and has been identified as a strong risk factor for eventual cerebral infarction[4]. Several studies have demonstrated that DCI can occur in brain regions unaffected by angiographic large vessel vasospasm thus suggesting that other processes such as distal cerebral vessel dysfunction, microthrombi formation and spreading cortical depression may also contribute to this phenomenon [5–7]. For decades the standard of care for DCI in the setting of SAH included induced hypertension, hypervolemia and hemodilution, so called “triple-H” therapy. Despite the efficacy of this treatment modality, some cases prove to be medically refractory, often in the setting of severe angiographic vasospasm, when endovascular treatment (EVT) with either catheter directed intraarterial (IA) vasodilator injection or percutaneous transluminal angioplasty (PTA) are warranted [3,8].

Several IA vasodilators have been reported in the literature for the treatment of cerebral vasospasm in SAH with variable efficacy and no clear consensus exists on how to gauge a successful treatment effect, particularly for distal vasospasm [9]. A timely detection of vascular changes is needed to assess the status of cerebral vessels, determine the need for ongoing medical or surgical intervention, and evaluate the effectiveness of interventions provided. At the University of California San Francisco (UCSF) Medical Center, verapamil is primarily used for EVT of distal cerebral vasospasm (CVS) and the goal of this retrospective study was to summarize the clinical procedure of IA verapamil injection for vasospasm including the infusion dosing, vasospastic territory and number of injections. Furthermore, we propose a novel method for continuous intra-procedural assessment of EVT for CVS. We premise that distal cerebral arterial changes induce a consistent pattern of morphological changes in the intracranial pressure (ICP) pulse. To accomplish this we used a previously published algorithm that was based upon a template of observed ICP pulse

morphological changes associated with cerebral arterial vasodilation and vasoconstriction [10–13]. Based on this algorithm, two parameters were developed to assess the likelihood of cerebral vasodilation and vasoconstriction from ICP signals recorded at bedside and during EVT [10,12], respectively. These two parameters are termed vasodilation index (VDI) and vasoconstriction index (VCI).

## METHODS

### Study population and data collection

192 recordings from 115 patients suffering aneurysmal SAH who underwent EVT for CVS between March 2017 and March 2019 at the UCSF medical center were reviewed. The study was approved by the local Ethics Committee with a waiver of patient consent because the study only analyzed existing data in a retrospective fashion.

The decisions to treat these patients in the Neuro Interventional Radiology (NIR) were completely based on clinicians' judgement as part of standard care at UCSF. Angiographic CVS was confirmed with digital subtraction angiography (DSA) and treated with (1) PTA for proximal vasospasm; and 2) IA verapamil injection for distal vasospasm in the main artery dedicated to the vasospastic territory (anterior cerebral artery [ACA], middle cerebral artery [MCA], internal carotid artery [ICA], vertebral artery [VERT], common carotid artery [CCA], Fig 1B). Infusion could be repeated in the same territory if an incomplete reversal was observed. Intra-arterial verapamil could also be repeated in a different territory in situations where there was extensive vasospasm. Verapamil was selectively administered through a diagnostic catheter (5F; Codman Neurovascular, Miami Lakes, Florida) or via an SL-10 micro-catheter (Stryker Neurovascular, CA, USA) with a dosage of 1 mg to 20 mg. Verapamil was diluted in normal saline to a final concentration of 0.5 mg/mL and infused at a rate of 0.5 mg per minute. Among all the 192 recordings, only 27 recordings from 21 patients had ICP recordings with good quality waveforms and they were analyzed in this study to detect vascular changes in response to verapamil injection. The rest of patients either did not have ICP recordings due to lack of external ventricular drain (EVD) or their EVD was open throughout the procedure causing loss of valid ICP waveform recordings. Five recordings had percutaneous transluminal angioplasty (PTA), including 4 cases with PTA in MCA and 1 case with PTA in vertebral and basilar artery. The details of verapamil injection and PTA treatment were summarized in Supplementary Table 1.

Among 27 recordings with analyzable ICP signals, 22 recordings had simultaneous, continuous, invasive arterial blood pressure measurement through femoral artery or radial artery. All signals were sampled at 240 Hz and recorded using BedMaster software (Excel Medical, Jupiter, Florida, USA). Parameters collected included: Patients' Hunt & Hess Grade[14], modified Fisher Score[15], the infusion dosage of each verapamil injection, vasospastic territory, number of injections, duration of each injection, and the time intervals between adjacent injections. We conducted a chart review of all transcranial doppler (TCD) recordings of cerebral blood flow velocity (CBFV) in the bilateral MCA, ACA and ICA in the three days prior to and after EVT.

### Morphological Clustering and Analysis of Intracranial Pulse (MOCAIP)

In this study, we applied a validated algorithm, Morphological Clustering and Analysis of ICP (MOCAIP) algorithm, to extract the morphological features of an ICP pulse including pulse amplitude, time intervals among subpeaks (P1, P2, P3), curvature, slope, and decay time constants (shown in Supplementary doc 1) [10,12,13,16,17,]. In general, a sequence of consecutive raw ICP pulses were segmented and then clustered into distinct groups based on their morphological distance; by doing this, the noise and artifacts can be excluded; then the largest cluster is identified and the averaged pulse of this largest cluster is calculated and termed dominant ICP pulse[18]; Thirdly, a reference library of validated ICP pulses is used to recognize legitimate dominant pulses [12], and then the MOCAIP algorithm performs a comprehensive search for all landmark points on an ICP pulse and use them as candidates for designating the three subpeaks. Finally, the best designation of the three well-recognized ICP subpeaks are obtained for each validated pulse [16]. As Supplementary document 1 summarizes, 128 pulse morphological metrics are extracted using the identified subpeaks and troughs of the pulse. More details of the MOCAIP algorithm should be referred to our published work [12].

### Vasodilation and vasoconstriction index

In a previous study, we showed consistent changes of 72 features in morphological of ICP pulses during vasoconstriction and vasodilation in a carbon dioxide (CO2) challenge experiment [10,16]. These metrics are considered consistent because they show opposite changes in response to vasoconstriction and vasodilation, respectively. These 72 consistent MOCAIP metrics were saved as a template of expected characteristic ICP pulse morphological changes during cerebral vascular changes. By comparing the changes of MOCAIP metrics of ICP before and after verapamil injection, and match them with the template defined above, we can determine whether the cerebral vasculature is in a vasodilatory, a vasoconstrictive, or a neutral state. Specifically, a vasodilation index (VDI) can be calculated as

$$VDI = \frac{N\left((S_+ \cap T_+^D) \cap \left(T_+^D \cap T_-^C\right)\right) + N\left(\left(S_- \cap T_-^D\right) \cap \left(T_-^D \cap T_+^C\right)\right)}{N\left(T_+^D \cap T_-^C\right) + N\left(T_-^D \cap T_+^C\right)} \quad \text{(F1)}$$

In a similar way, a vasoconstriction index (VCI) can be calculated as

$$VCI = \frac{N\left((S_+ \cap T_+^C) \cap \left(T_+^C \cap T_-^D\right)\right) + N\left(\left(S_- \cap T_-^C\right) \cap \left(T_-^C \cap T_+^D\right)\right)}{N\left(T_+^D \cap T_-^C\right) + N\left(T_-^D \cap T_+^C\right)} \quad \text{(F2)}$$

where $S_+$ denotes a set of MOCAIP metrics showing positive change from baseline, $S_-$ a set of MOCAIP metrics showing negative change from the baseline, $T_+^C(T_-^C)$ a set of MOCAIP metrics in the template showing positive (negative) changes during a cerebral vasoconstriction phase, and $T_+^D\left(T_-^D\right)$ a set of MOCAIP metrics in the template showing positive (negative) changes during a cerebral vasodilation phase. A ∩ B refers to the

intersection of two sets. It should be noted that the range of VCI and VDI is between 0 and 1.

In this study, the VDI and VCI was calculated on a pulse by pulse basis. Six pulses before the first injection were randomly picked and used as a baseline to compare ICP pulse morphological changes. The average VDI/VCI that was derived from comparing each consecutive dominant ICP pulse to each of the six baseline ICP pulses was reported. In this way, we were able to smooth out the variations in VDI/VCI that are likely due to respiration. For more details of VCI/VDI calculation, please refer to our previous publications [10,12,13].

### Cerebral autoregulation parameter

Wavelet transform based phase difference (WTP) between ABP and ICP, in the low frequency of 0.005 Hz to 0.08 Hz was used to assess cerebral autoregulation [19–23]. Morlet mother wave was applied to extract the characteristics of arterial blood pressure (ABP) and ICP signals. The wavelet phase difference at each scale-frequency point was calculated, and wavelet transform coherence (WTC) was used as an indicator of a reliable phase relationship between input and output. Individual phase difference values with coherence higher than the threshold (0.48, decided through Monte Carlo simulations) were kept, while phase difference values with coherence lower than the threshold were deleted. The cosine of the wavelet phase difference, termed wPRx, was calculated as a practical solution to the problem of phase wrapping. Then the average value of cosine of wavelet phase difference along frequency at each time point was calculated. More details about the algorithm can be found in our previous publication [23]. The mean value of VCI, VDI and wPRx before, during and after verapamil injection was calculated.

### Statistical analysis

Statistical analysis was performed using the IBM SPSS Statistics (version 24, IBM, New York, USA) software. The mean values of VCI, VDI, ICP, wPRx and ABP of baseline, between the 1st and the 2nd injections, and between the 2nd and the 3rd injections were calculated. One-way ANOVA was used to test whether there is a significant difference in these parameters between at least two different time groups. If the $p$ value of one-way ANOVA was smaller than 0.05, an additional multiple comparison test (Bonferroni) was used to find out where the significant difference was located. Spearman rank-order correlation analysis were used to test the correlation between mean CBFV values (from ICA, ACA and MCA) and VCI, VDI, ICP and ABP. The $p$ value level of significance was 0.05 and all $p$ values were 2-sided.

## RESULTS

### Summary of clinical procedure of IA Verapamil injection

A total of 387 injections of verapamil were found among the 192 recordings, with two injections on average per procedure, ranging from 1–5 injections/procedure. Injections were administered through ICA (72.1%), VA (18.3%), CCA (5.7%), ACA (2.3%) and MCA (1.6%) with 46% on the right side and 54% on the left (Fig 1A). The dosage of each injection varied (mean dose of each injection: 9.17 ± 4.43 mg, mean ± SD), with most

injections being either 5 mg or 10 mg (Supplementary Figure 1A). Higher injected dose seems to have longer duration of vasodilatory effect, and results in longer time interval to the next injection, but the difference was not significant (Supplementary Figure 1B). There was significant heterogeneity in doses injected depending on which artery was selected, with CCA, ICA and ACA receiving higher doses than other arteries (Supplementary Figure 1C).

### VCI and VDI changes after Verapamil injection

Among all the 192 recordings, only 27 recordings from 21 patients have ICP recordings with high quality which were analyzed to detect vascular changes. The subjects include 8 males and 13 females, with median age at 58 ± 12.6 years old. The patient demographics are described in Supplementary Table 1.

Figure 2 shows an example of continuous VCI and VDI with three injections of verapamil. The statistical analysis of the 21 patients' recordings showed that VDI was significantly increased after the 1st injection (Mean ± SD: 0.50 ± 0.02, p=0.001) and the 2nd injection (0.52 ± 0.021, p=0.003) comparing with VDI at baseline (0.47 ± 0.017, Fig 3). The VCI was significantly lower after the first injection (0.47 ± 0.02) than VCI at baseline (27 recordings from 21 patients, 0.49 ± 0.02, p<0.001). ICP and ABP did not change after verapamil injection (p>0.05, Fig 3). Autoregulation did not show significant differences before and after verapamil injection (22 recordings from 19 patients, wPRx of baseline was 0.38 ± 0.08, wPRx after 1st injection was 0.45 ± 0.08, wPRx after the 2nd injection was 0.49 ± 0.09, p>0.05).

### The effects of different dosages of IA injection

In order to study whether VDI can be used to detect the effect of intra-arterial vasodilators continuously, we calculated the mean value of VDI every one minute, with the starting time anchored at the time of the first injection. As shown in Fig 4, VDI started to increase after the first injection of verapamil with larger doses (15 mg) conferring a more robust total increase in VDI. In addition, the duration of VDI increase also demonstrated a clear dose response such that higher doses of verapamil led to a more prolonged response. There were no observed changes in ICP in response to increasing doses of verapamil (Supplementary Fig 2).

### TCD results

Insonation of the MCA and ACA with TCD demonstrated an increase in CBFV days prior to IA injection with verapamil which was then followed by a clear decrease after EVT (Supplementary Fig 3A). Conversely, these trends were not clearly observed in response to verapamil treatment when measuring velocities within the ICA (Supplementary Fig 3B–3C). Baseline VCI demonstrated a linear relationship with CBFV of MCA prior to verapamil injection on the day of injection(r=0.47, p<0.001, Supplementary Fig 3D).

## DISCUSSION

DCI is the most important in-hospital modifiable risk factor for poor outcome after aneurysmal SAH and EVT represents an indispensable treatment modality in the

armamentarium of strategies to prevent irreversible cerebral injury from severe hypoperfusion[3,4]. Despite clinical evidence that IA vasodilators can increase oxygenation to areas of critical cerebral ischemia and improve neurologic function in patients with DCI, there is no consensus on how to best gauge an adequate response to therapy or stratify which patients may benefit from ongoing treatments[24,25]. In this study, we introduced a novel method for continuous assessment of cerebral vascular responses to IA vasodilator admission in aneurysmal SAH patients during EVT. Our results demonstrate that VDI increases significantly after verapamil administration and remains elevated in a dose dependent manner.

The shape of ICP is determined by the interaction between vascular pulses and intracranial compartment[26,27]. Previous experiment studies already reported the arterial origins of ICP pulses by ligation of different cerebral arterial branches to isolate the contributions of specific sources [26,28,29]. Meanwhile, studies on mathematical modeling of ICP dynamics and cerebral hemodynamics also apply the principle of conservation of mass to model the relationship between cerebrospinal fluid compartment and cerebral blood compartment [30,31]. In general, researchers suggest that the first peak of ICP waveform (P1) mainly reflects the pulsations of large intracranial conductive arteries, the second peak (P2) might represent cerebral vascular pulsations in capillaries and brain parenchymal; the P1/P2 ration reflects compliance of the brain and the third peak (P3) is mainly related with venous pulsation [26,28,29]. In current mathematical models of ICP pulses, six major branches of cerebral arteries (left/right MCA, left/right ACA, left/right PCA) are the main source of ICP pulses. Theoretically, cerebral arterial vasodilation and vasoconstriction will alter the shape of arterial pulses, e.g., through the amplification or damping of reflected waves, resulting in changes in ICP pulse waveforms. This is the premise of our study.

In work done by Hu and colleagues, an advanced algorithm known as the Morphological Cluster and Analysis of Intracranial Pressure (MOCAIP) was developed to extract specific morphologic features from an ICP waveform. As explained above, the ICP pulse is mainly derived from transmitted arterial pulses, the change of arterial pulse waveform due to active cerebral vasodilation and vasoconstriction will be reflected in ICP pulse waveforms [32]. Using MOCAIP technology, Asgari et al found reliable changes in ICP MOCAIP morphology in response to CO2 inhalation and with morphologic template matching method were able to develop a standardized metric for assessment of VCI and VDI [11,16]. These indices have been validated across several different patient cohorts and have shed insights on autoregulation and dynamic cerebral vascular changes which occur after CSF drainage [11,13]. This study is the first to employ a similar template matching method for assessment of cerebral blood vessel dilation and constriction in response to EVT in patients with aneurysmal SAH and vasospasm.

Cerebral vasospasm is characterized radiographically by the presence of luminal narrowing of the large intracerebral arteries and develops in 30–50% of patients who are admitted with aneurysmal SAH [2,4]. Though angiographic vasospasm is highly correlated with the development of DCI and cerebral infarction, up to a quarter of patients develop evidence of regional hypoperfusion without large vessel vasospasm indicating that other mechanisms must be involved[5]. Using positron emission tomography (PET), Yundt et al imaged patients

with carotid artery occlusion and found increased cerebral blood volume (CBV) consistent with maximal vasodilation in parenchymal vessels, however in SAH patients with vasospasm there was a significant decrease in CBV suggesting impaired autoregulation due to pathologic vasoconstriction of the small arteries and arterioles [33]. This small vessel vasospasm has also been described using analysis of the time-density curve of contrast media in the parenchymal vessels of patients undergoing digital subtraction angiography (DSA), termed cerebral circulatory time (CCT), which demonstrates a strong inverse correlation with regional CBF even without large vessel vasospasm and can be normalized after administration of IA papaverine, further supporting the notion that small vessel dysfunction contributes to the development of DCI [34,35]. Using the MOCAIP algorithm we are able to evaluate cerebrovascular resistance across the entire intracranial compartment which likely encompasses both proximal and distal vessel changes. Both VCI and VDI were devised using control patients with known cerebral vasoconstriction and vasodilation due to CO2 challenge and hyperventilation respectively and since the majority of autoregulatory changes are mediated at the level of precapillary arterioles and small vessels, these indices may provide a unique window into dynamic alterations in small vessel resistance [16,36,37]. In the context of SAH such tools may prove useful for continuous assessment of vasospasm, including distal vessel changes, as a way to monitor for early DCI and target interventions to prevent cerebral infarction.

Aggressive EVT including IA vasodilator injection and PTA are indispensable treatment options for improving CBF to areas of severe vasospasm thus preventing irreversible infarction and may serve to improve long-term neurologic functional status [38,39]. Despite the proposed benefits of EVT, rare though potential serious complications can occur including vessel perforation, hemorrhage and thrombotic events and there is no clear consensus on which particular set of patient characteristics to which these procedures may be of benefit[9,39]. PTA is thought to disrupt vascular smooth muscle function and typically leads to a durable dilation of vessels in which it is employed, with rare recurrence of vasospasm, however it can only be utilized in large caliber vessels with diameters ≥ 2mm therefore limiting its utility in the treatment of distal or small vessel vasospasm[9]. IA vasodilators are a compelling treatment modality for distal vasospasm however there are several available agents with differing mechanisms of action including verapamil, milrinone and nicardipine, and no comparative studies are available[39]. Among the most routinely used IA vasodilators the doses administered are commonly left to the discretion of the treating physician based off the degree of angiographic vasospasm and no current method exists to allow for titration. In studies using IA calcium channel blocking agents, there are inconsistencies between the radiographic changes and clinical improvement with some reports demonstrating robust resolution of angiographic vasospasm without significant neurologic improvement whereas others have found the opposite association [3,40–42]. These discrepant findings indicate that radiographic resolution of vasospasm in the angiography suite itself is not a sensitive nor specific marker to gauge the efficacy of IA vasodilator treatment and more reliable and objective measures are needed. In this study, we collected the dosage, target vessels, and time intervals between consecutive injections from 387 EVT procedures and found a predictable change in VDI in response to vasodilator therapy. With higher doses of verapamil there was a significant increase in the magnitude of VDI rise as well as more

prolonged effect. Using continuous ICP waveform analysis, it may be possible to rapidly gauge an individual patient's physiologic response to vasodilator therapy and use specific treatment thresholds based off VDI to guide subsequent interventions. Further studies are now warranted to correlate particular VDI thresholds with CBF values sufficient to prevent infarction in the setting of vasospasm related to aneurysmal SAH.

In this pilot study involving 21 patients with aneurysmal SAH and angiographic vasospasm we evaluated daily TCD recordings and found that CBFV increased in the days leading up to EVT which is in accordance with Besheli et al [43]. Moreover, the fact that the MCA and ACA seemed to conform to a similar response while ICA did not change would further support that verapamil affects the distal than the proximal arteries. Interestingly, CBFV demonstrated a linear relationship with VCI suggesting that the latter may be used as a global marker surrogate marker of cerebrovascular resistance and monitor for the occurrence of vasospasm in a continuous manor. The majority verapamil injections were performed in the anterior circulation (88%, 51/58) and only one patient had an infusion solely in the vertebral artery making it challenging to assess whether similar waveform alterations can be expected in the posterior circulation. Although no statistically significant changes in CA were observed in relation to verapamil administration, the mean value of wPRx showed an increased trend, from 0.38 ± 0.08 at baseline to 0.45 ± 0.08 after the first injection and 0.49 ± 0.09 after the second injection. This overall increased trend in wPRx is interesting in that it may suggest blunted autoregulatory capacity following verapamil administration due to vasodilation. Importantly, our results demonstrated no changes in ICP following vasodilator administration which has rarely been reported in the literature, most often with papaverine [3,9].

Our study has several important limitations. First, we have only included 27 recordings from 21 aneurysmal SAH patients, which had ICP recordings of high enough quality to be analyzed using MOCAIP. This method requires validation using a larger cohort of patients with SAH. Secondly, it would be ideal if we can correlate VDI and VCI indices with angiographic response after verapamil injection. However, in this study, post-verapamil angiograms were not routinely performed in all cases in order to reduce patient contrast and x-ray dose. Only in 5 cases who need additional verapamil or PTA, post-verapamil angiograms were performed and mild improvement in intracranial vessel caliber was noticed post verapamil infusion. In these cases, we did see an increase in VDI after the first and second injection of verapamil comparing to the baseline. In the following studies, we will need to systematically record the result of post-verapamil angiograms or results of diagnostic studies of CBF such as PET or perfusion imaging to further study these potential correlations. Furthermore, VCI and VDI have not been evaluated in association with clinical improvement following intervention nor the risk of developing DCI and cerebral infarction. Finally, in our study we only evaluated a response to verapamil and it will be important to ascertain if similar changes occur in response to other vasodilators (e.g. Milrinone, Nimodipine) or PTA prior to applying these parameters to clinical use.

## CONCLUSION

In this retrospective study we validated the use of the VDI/VCI algorithm for continuous assessment of vascular change during EVT in patients with vasospasm secondary to aneurysmal SAH. Following infusion of IA verapamil there is a significant decrease in VCI and increase in VDI which responds in a dose dependent manor. These indices require further validation in larger studies though may prove useful for monitoring aneurysmal SAH patients for vasospasm and titrating EVT.

## Supplementary Material

Refer to Web version on PubMed Central for supplementary material.

## Acknowledgments

FUNDING STATEMENT

This work was supported by National Institutes of Health grant number [R01NS089771A1] and Middle Career Scientist Award, UCSF Institute for Computational Health Sciences.

## REFERENCES

1. Johnston SC, Selvin S, Gress DR. The burden, trends, and demographics of mortality from subarachnoid hemorrhage. Neurology. 1998;50(5):1413–1418. [PubMed: 9595997]
2. Frontera JA, Fernandez A, Schmidt JM, et al. Defining vasospasm after subarachnoid hemorrhage: What is the most clinically relevant definition? Stroke. 2009;4:1963–8.
3. Jun P, Ko NU, English JD, et al. Endovascular treatment of medically refractory cerebral vasospasm following aneurysmal subarachnoid hemorrhage. AJNR Am J Neuroradiol. 2010;31:1911–6. [PubMed: 20616179]
4. Rabinstein AA, Friedman JA, Weigand SD, et al. Predictors of cerebral infarction in aneurysmal subarachnoid hemorrhage. Stroke. 2004;35:1862–6. [PubMed: 15218156]
5. Dhar R, Scalfani MT, Blackburn S, Zazulia AR, Videen T, Diringer M. Relationship between angiographic vasospasm and regional hypoperfusion in aneurysmal subarachnoid hemorrhage. Stroke. 2012;43:1788–94. [PubMed: 22492520]
6. Stein SC, Browne KD, Chen XH, Smith DH, Graham DI. Thromboembolism and delayed cerebral ischemia after subarachnoid hemorrhage: An autopsy study. Neurosurgery. 2006;59:781–7. [PubMed: 16915120]
7. Woitzik J, Dreier JP, Hecht N, et al. Delayed cerebral ischemia and spreading depolarization in absence of angiographic vasospasm after subarachnoid hemorrhage. J Cereb Blood Flow Metab. 2012;32:203–12. [PubMed: 22146193]
8. Kimball MM, Velat GJ, Hoh BL, Participants in the International Multi-Disciplinary Consensus Conference on the Critical Care Management of Subarachnoid Hemorrhage. Critical care guidelines on the endovascular management of cerebral vasospasm. Neurocrit Care. 2011;15:336–41. [PubMed: 21761272]
9. Pierot L, Aggour M, Moret J. Vasospasm after aneurysmal subarachnoid hemorrhage: Recent advances in endovascular management. Curr Opin Crit Care. 2010;16:110–6. [PubMed: 20098322]
10. Asgari S, Bergsneider M, Hamilton R, Vespa P, Hu X. Consistent changes in intracranial pressure waveform morphology induced by acute hypercapnic cerebral vasodilatation. Neurocrit Care. 2011;15(1):55–62. [PubMed: 21052864]
11. Asgari S, Vespa P, Bergsneider M, Hu X. Lack of consistent intracranial pressure pulse morphological changes during episodes of microdialysis lactate/pyruvate ratio increase. Physiol Meas. 2011;32(10):1639–1651. [PubMed: 21904021]

12. Hu X, Xu P, Scalzo F, Vespa P, Bergsneider M. Morphological clustering and analysis of continuous intracranial pressure. IEEE Trans Biomed Eng. 2009;56(3):696–705. [PubMed: 19272879]
13. Liu X, Zimmermann LL, Ho N, Vespa P, Liao X, Hu X. Cerebral Vascular Changes During Acute Intracranial Pressure Drop. Neurocritical Care. 2018.
14. Hunt WE, Hess RM. Surgical Risk as Related to Time of Intervention in the Repair of Intracranial Aneurysms. J Neurosurg. 2009;28:14–20.
15. Fisher CM, Kistler JP, Davis JM. Relation of cerebral vasospasm to subarachnoid hemorrhage visualized by computerized tomographic scanning. Neurosurgery. 1980;6:1–9. [PubMed: 7354892]
16. Asgari S, Gonzalez N, Subudhi AW, et al. Continuous Detection of Cerebral Vasodilatation and Vasoconstriction Using Intracranial Pulse Morphological Template Matching. PLoS One. 2012;7(11):e50795. [PubMed: 23226385]
17. Hu X, Xu P, Lee DJ, Vespa P, Baldwin K, Bergsneider M. An algorithm for extracting intracranial pressure latency relative to electrocardiogram R wave. Physiol Meas. 2008;29(4):459–471. [PubMed: 18354246]
18. Hu X, Xu P, Asgari S, Vespa P, Bergsneider M. Forecasting ICP elevation based on prescient changes of intracranial pressure waveform morphology. IEEE Trans Biomed Eng. 2010;57(5):1070–1078. [PubMed: 20659820]
19. Grinsted a., Moore JC, Jevrejeva S. Application of the cross wavelet transform and wavelet coherence to geophysical time series. Nonlinear Process Geophys. 2004;11(5/6):561–566.
20. Kvandal P, Sheppard L, Landsverk SA, Stefanovska A, Kirkeboen KA. Impaired cerebrovascular reactivity after acute traumatic brain injury can be detected by wavelet phase coherence analysis of the intracranial and arterial blood pressure signals. J Clin Monit Comput. 2013;27(4):375–383. [PubMed: 23748602]
21. Liu X, Czosnyka M, Donnelly J, et al. Wavelet pressure reactivity index: A validation study. J Physiol. 2018;596:2797–809. [PubMed: 29665012]
22. Tian F, Tarumi T, Liu H, Zhang R, Chalak L. Wavelet coherence analysis of dynamic cerebral autoregulation in neonatal hypoxic-ischemic encephalopathy. NeuroImage Clin. 2016;11:124–132. [PubMed: 26937380]
23. Liu X, Donnelly J, Czosnyka M, et al. Cerebrovascular pressure reactivity monitoring using wavelet analysis in traumatic brain injury patients: A retrospective study. PLOS Med. 2017;14(7):e1002348. [PubMed: 28742798]
24. Albanna W, Weiss M, Müller M, et al. Endovascular rescue therapies for refractory vasospasm after subarachnoid hemorrhage: A prospective evaluation study using multimodal, continuous event neuromonitoring. Clin Neurosurg. 2017;80:942–9.
25. Badjatia N, Topcuoglu MA, Pryor JC, et al. Preliminary experience with intra-arterial nicardipine as a treatment for cerebral vasospasm. Am J Neuroradiol. 2004;25:819–26. [PubMed: 15140728]
26. Hamilton R, Baldwin K, Fuller J, Vespa P, Hu X, Bergsneider M. Intracranial pressure pulse waveform correlates with aqueductal cerebrospinal fluid stroke volume. J Appl Physiol. 2012.
27. Carrera E, Kim DJ, Castellani G, et al. What shapes pulse amplitude of intracranial pressure? J Neurotrauma. 2010.
28. Hirai O, Handa H, Ishikawa M, Kim SH. Epidural pulse waveform as an indicator of intracranial pressure dynamics. Surg Neurol. 1984.
29. Adolph RJ, Fukusumi H, Fowler NO. Origin of cerebrospinal fluid pulsations. Am J Physiol. 1967.
30. Ryu J, Hu X, Shadden SC. A Coupled lumped-parameter and distributed network model for cerebral pulse-wave hemodynamics. J Biomech Eng. 2015.
31. Ursino M, Lodi CA. Interaction among autoregulation, CO2 reactivity, and intracranial pressure: A mathematical model. Am J Physiol - Hear Circ Physiol. 1998.
32. Hu X, Glenn T, Scalzo F, et al. Intracranial pressure pulse morphological features improved detection of decreased cerebral blood flow. Physiol Meas. 2010;31(5):679–695. [PubMed: 20348611]
33. Yundt KD, Grubb RL, Diringer MN, Powers WJ. Autoregulatory Vasodilation of Parenchymal Vessels is Impaired during Cerebral Vasospasm. J Cereb Blood Flow Metab. 1998;18(4):419–24. [PubMed: 9538907]

34. Ohkuma H, Manabe H, Tanaka M, Suzuki S. Impact of cerebral microcirculatory changes on cerebral blood flow during cerebral vasospasm after aneurysmal subarachnoid hemorrhage. Stroke. 2000;31:1621–7. [PubMed: 10884463]

35. Touho H. Hemodynamic evaluation with dynamic DSA during the treatment of cerebral vasospasm: A retrospective study. Surg Neurol. 1995;44:63–73. [PubMed: 7482257]

36. Muizelaar JP, Poel H van der, Li ZC, van der Poel HG, Kontos HA, Levasseur JE. Pial arteriolar vessel diameter and CO2 reactivity during prolonged hyperventilation in the rabbit. J Neurosurg. 1988;69:923–7. [PubMed: 3142972]

37. Willie CK, Macleod DB, Shaw AD, et al. Regional brain blood flow in man during acute changes in arterial blood gases. J Physiol. 2012;590:3261–75. [PubMed: 22495584]

38. Mortimer AM, Steinfort B, Faulder K, et al. The detrimental clinical impact of severe angiographic vasospasm may be diminished by maximal medical therapy and intensive endovascular treatment. J Neurointerv Surg. 2015;7:881–7. [PubMed: 25304500]

39. Venkatraman A, Khawaja AM, Gupta S, et al. Intra-Arterial vasodilators for vasospasm following aneurysmal subarachnoid hemorrhage: A meta-Analysis. J Neurointerv Surg. 2018;10:380–7. [PubMed: 28663521]

40. Biondi A, Ricciardi GK, Puybasset L, et al. Intra-arterial nimodipine for the treatment of symptomatic cerebral vasospasm after aneurysmal subarachnoid hemorrhage: Preliminary results. Am J Neuroradiol. 2004.

41. Feng L, Fitzsimmons BF, Young WL, et al. Intraarterially administered verapamil as adjunct therapy for cerebral vasospasm: Safety and 2-year experience. Am J Neuroradiol. 2002;23:1284–90. [PubMed: 12223366]

42. Mazumdar A, Rivet DJ, Derdeyn CP, Cross DT, Moran CJ. Effect of intraarterial verapamil on the diameter of vasospastic intracranial arteries in patients with cerebral vasospasm. Neurosurg Focus. 2006;21:E15.

43. Besheli LD, Tan CO, Bell DL, Hirsch JA, Gupta R. Temporal evolution of vasospasm and clinical outcome after intra-arterial vasodilator therapy in patients with aneurysmal subarachnoid hemorrhage. PLoS One. 2017;12:e0174676.

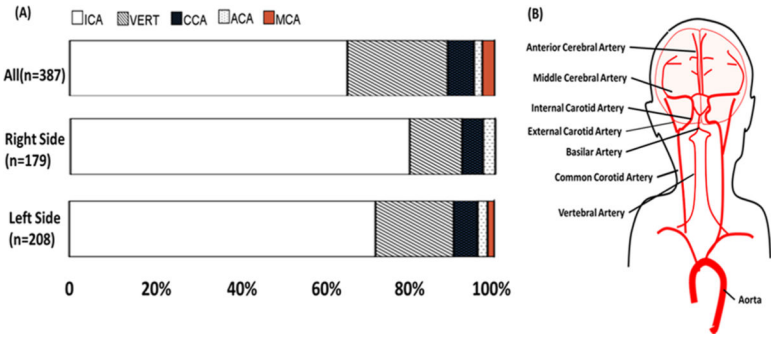


**Fig 1.**

A) The percentage of verapamil injection in each artery. B) The anatomy of the arteries that has endovascular treatment in our study. ACA: anterior cerebral artery; MCA: middle cerebral artery; ICA: internal carotid; ECA: external carotid artery; BA: basilar artery; CCA: common carotid artery; VERT: vertebral artery.

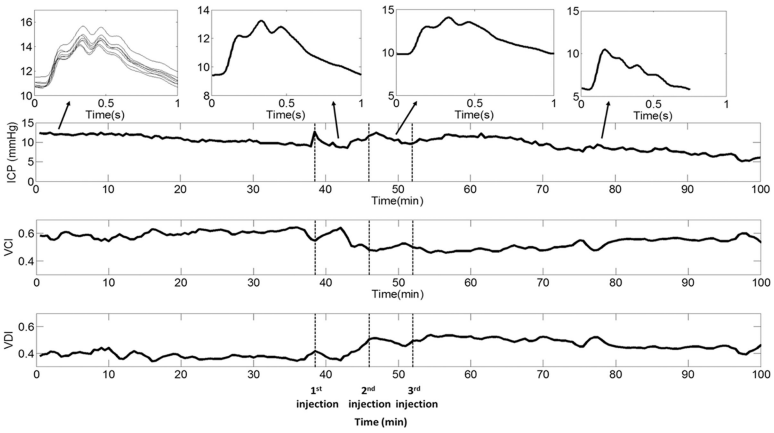


**Fig 2.**

An example VDI, VCI changes after verapamil injection. The three vertical, dot lines represent three injections of verapamil medicine. The four small charts in the upper panel represent dominant ICP pulses at baseline (6 dominant pulses that were selected as baseline pulses to be compared to for VCI and VDI calculation), after the 1st injection, after the 2nd injection, and after the 3rd injection. ICP: intracranial pressure, VCI: vasoconstriction index, VDI: vasodilation index.

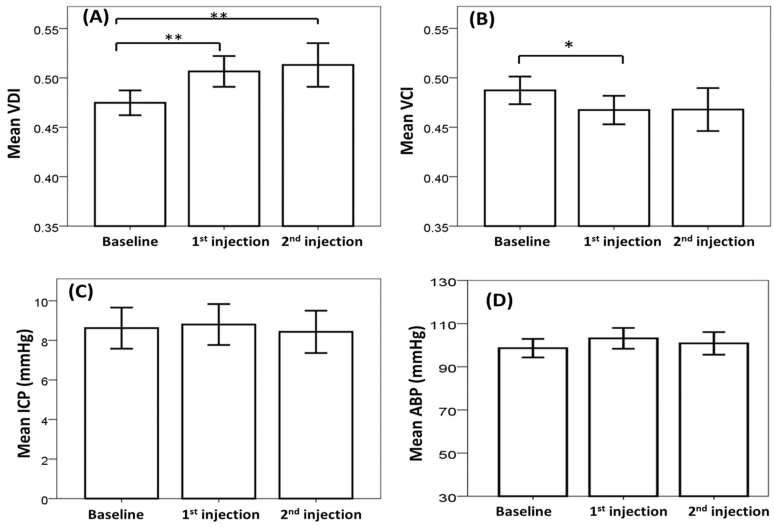


**Fig 3.**

Mean values of VCI, VDI, ICP and ABP before and after injection of verapamil medicine. ICP: intracranial pressure, VCI: vasoconstriction index, VDI: vasodilation index. ABP: arterial blood pressure. P<0.05 was considered to be significant. * means p<0.05; ** means p<0.01.

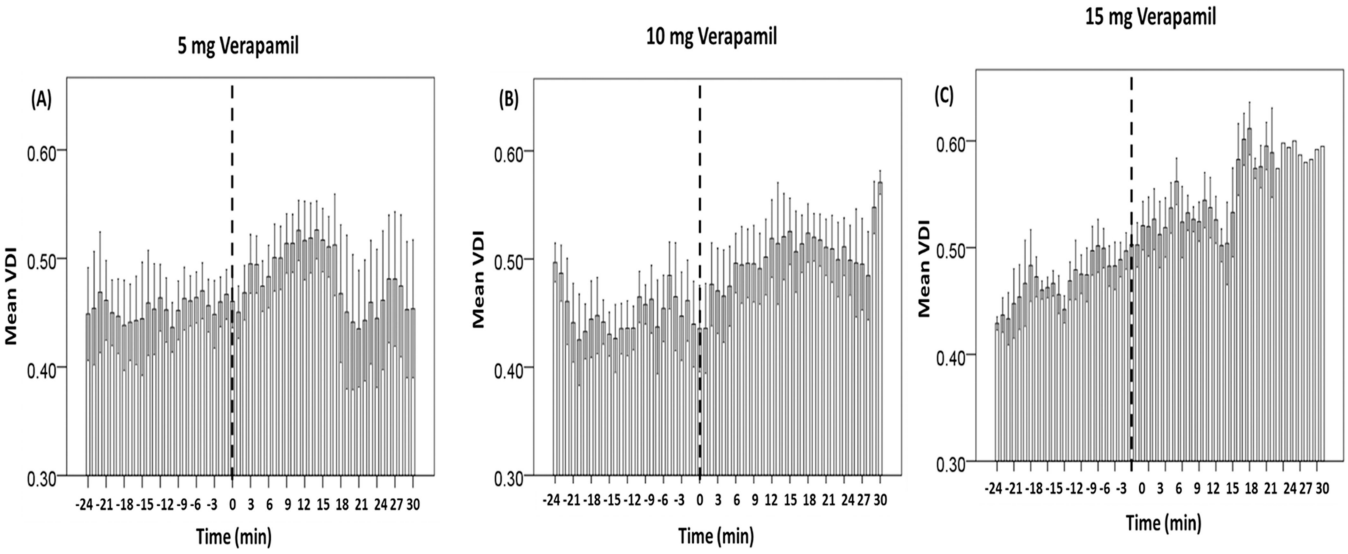


**Fig 4.**

VDI changes along time with injection of different dosage. Time 0 refers to the time point when the verapamil was first injected. VDI: vasodilation index.